Use of standard fluorescence microscopy to assess modifications in the plasma membrane potential and in the intracellular concentration of inorganic ions in cultured cells

Silvia Chifflet[*,1], and **Julio A. Hernández**[2]

[1] Departamento de Bioquímica, Facultad de Medicina, Universidad de la República, Gral. Flores 2125, 11800 Montevideo, Uruguay.
[2] Sección Biofísica, Facultad de Ciencias, Universidad de la República, Iguá s/n esq. Mataojo, 11400 Montevideo, Uruguay.

As an alternative to electrophysiological procedures, fluorescent probes have been widely used to assess modifications in the plasma membrane potential (PMP) of living cells, mostly via spectrophotometric or spectrofluorimetric analysis of samples of suspended cells. Another suggested procedure for the quantitative study of PMP changes using fluorescent probes utilizes confocal microscopy and image analysis of cells loaded with potentiometric probes. A modification of this latter procedure employs standard fluorescent microscopy and image analysis (FM-IA). We have used this methodology to study modifications in the PMP and intracellular ionic concentrations for the case of cultured epithelial cells. In this chapter we describe the FM-IA method, illustrate its utilization with examples taken from our published work and discuss possible applications and shortcomings.

Keywords fluorescence microscopy; image analysis; fluorescent probes; plasma membrane potential; intracellular ionic concentrations

1. Introduction

The plasma membrane potential and the intracellular concentrations of inorganic ions represent relevant physiological variables, subject to regulatory mechanisms [1-4] and involved in diverse cellular signalling paths. [5-7]. The in vivo measurement of the modifications undergone by these variables under diverse experimental conditions has therefore represented a major methodological goal of cell physiology. For the case of the plasma membrane potential (PMP), an alternative to the classical electrophysiological procedures was provided by the employment of diverse organic molecules as potentiometric probes [8] [9]. The non-destructive character of this approach represented an obvious benefit with respect to electrophysiological techniques, which occasionally may produce severe alterations in the cell membrane and, consequently, leakage of ions [8] and relevant metabolites [10]. In the earlier stages the use of potentiometric probes was restricted to spectrophotometric or spectrofluorimetric analysis of samples of suspended cells [11, 12]. This represented a serious limitation to the use of this type of probes, since only free circulating cells or experimentally suspended adherent cells could be investigated. This methodology was hence successfully applied to assess PMP modifications in cells such as lymphocytes [13], neutrophils [14, 15], HeLa cells [16] and adrenal chromaffin cells [17]. However, in multicellular organisms the majority of the cells constitute structures where the cells establish firm contacts between them or with the extracellular matrix. The experimental breakage of these adhesions to obtain samples of independently suspended cells for analytical purposes therefore constitutes a major perturbation of their physiological conditions. This is typically the case, for instance, of epithelial cells that in vivo establish uni or multicellular layers of tightly connected cells. The protective and transport properties of epithelia strongly depend upon the conservation of intercellular junctions [18, 19]. More recently, the employment of fluorescence microscopy and, particularly, the advent of confocal laser scanning microscopy (CLSM) permitted a direct study of the PMP

[*] Corresponding author: e-mail: schiffle@mednet.org.uy, Phone: +5982 9243414 ext.3406

modifications in adherent cells [20, 21]. Among other advantages, the introduction of this methodology allowed the observation of modifications in individual cells, whereas the fluorimetric or spectrophotometric studies of suspended cells are only able to obtain average measurements of the overall cell population. In particular, the use of probes of the oxonol family, due to their anionic nature, permitted to isolate the PMP signal from that of the mitochondria and obtain reliable calibration curves [21, 22].

We have employed a modification of the CLSM analysis of fluorescent probe signal to study relative changes in the PMP by the use of standard fluorescent microscopy and image analysis (FM-IA) for the case of cultured epithelial cells [23-25]. Although the CLSM allows the visualization of a detailed spatial distribution of the dyes, for the study of global physiological properties standard fluorescent microscopy also yields accurate results. In addition, its more general availability makes it a convenient and practical procedure. We used the FM-IA methodology to demonstrate that non-specific modifications in the PMP of cultured epithelial cells, achieved by the incorporation of ionophores or by manipulations in the composition of the bathing media, determine characteristic reorganizations of the cytoskeleton of cultured epithelial cells [23, 25]. For the analysis, we employed the potentiometric dye oxnol V. As an example of the possible physiological relevance of those findings, we determined that depolarization of the PMP occurs in the border cells of wounds in epithelia and that this depolarization is crucial to achieve the cytoskeletal modifications necessary for the healing process [24]. In this latter and current work we also applied the FM-IA method to the case of probes for calcium and sodium ions. Although the method is, in principle, limited to reveal relative modifications in the PMP or in the ionic concentrations and not suitable for precise determinations of absolute values, it nevertheless permitted to produce calibration curves yielding quantitative results in fair approximation to available literature [24]. In this chapter we describe the FM-IA method, illustrate its utilization with examples taken from our published work and discuss possible applications and shortcomings.

2. Experimental procedures

In this section we briefly describe the fundamentals and method of study of modifications in the plasma membrane potential and intracellular concentration of sodium by FM-IA employing, for illustrative purposes, work performed in our laboratory on bovine corneal endothelial cells and other eye epithelia in culture [23-25].

2.1 Cell cultures and experimental modifications of the plasma membrane potential

Cultures of bovine corneal endothelial cells (BCE cells) were obtained as described [25]. For the studies, cell monolayers grown in Minimal Essential Medium (MEM) containing 10 % fetal calf serum were plated on hand-cut square glass coverslips. Experiments were performed at least five days after the cells had achieved visual confluence.

The manipulations performed to modify the PMP can be interpreted with the aid of the Goldman-Hodgkin-Katz equation [26]:

$$\Delta V_m = V_i - V_o = \frac{RT}{F} \ln \frac{P_K \left[K^+\right]_o + P_{Na} \left[Na^+\right]_o}{P_K \left[K^+\right]_i + P_{Na} \left[Na^+\right]_i} \ ,$$

where V_i and V_o are the electrical potentials at the intracellular and extracellular compartments; P_K and P_{Na} are the permeability coefficients of potassium and sodium across the plasma membrane; $[K^+]_i$, $[Na^+]_i$, $[K^+]_o$, $[Na^+]_o$ are the corresponding ionic concentrations, and where F is Faraday's constant, R the gas constant and T the absolute temperature.

PMP depolarization was produced by incorporation of gramicidin D to the incubation media or by replacement of extracellular sodium chloride by potassium gluconate. Gramicidin D is a channel-forming

peptide selective to monovalent cations [27]. At the conditions usually encountered in most non-excitable animal cells, where potassium is close and sodium very far to electrochemical equilibrium, respectively, incorporation of gramicidin to the plasma membrane produces PMP depolarization and a raise in the intracellular sodium concentration, as a consequence of the increase in sodium permeability (P_{Na}). For the experiments, gramicidin D solutions were prepared from a 10 mg/ml stock solution in dimethyl sulfoxide (DMSO) kept at -20ºC. This solution was diluted in the corresponding buffer immediately before each experiment, to a final concentration between 1 and 10 μg/ml. Controls were performed with DMSO alone to discard possible effects of this solvent.

PMP depolarization was also provoked by replacement of extracellular sodium by potassium. In this case, the increase in extracellular potassium ($[K^+]_o$) decreases the electrochemical gradient of this ion. On the contrary, PMP hyperpolarization was achieved by replacement of extracellular sodium by choline, a non-diffusive cation. In this case, the electrochemical gradient of sodium decreases as a consequence of the decrease in extracellular sodium concentration ($[Na^+]_o$).

2.2 Potentiometric probes and determination of changes in the plasma membrane potential

Potentiometric probes fall into two categories, fast and slow, according to the speed of the PMP-dependent optical changes [11]. The magnitude of the optical responses of the slow probes may reach up to 34% per 100 mV and is therefore much larger than that of fast-response probes, which is typically about 2-10% per 100 mV [28]. Slow-response probes, which include anionic oxonols, reveal changes in the order of minutes and are appropriate for studying modifications in average membrane potentials of nonexcitable cells [11, 28]. The members of the oxonol family have been shown to partition between the cell and the extracellular medium in a PMP-dependent manner [11, 29], such that an increase in the oxonol fluorescence intensity of the cell corresponds to membrane depolarization [29]. Due to their negative charge, these dyes accumulate in the vesicular compartment [21, 30]. Thus, one possible artifact in the membrane potential estimation by these dyes may arise when the experimental manipulations provoke an increase in the number or size of intracellular vesicles. The diverse members of the oxonol family exhibit different physicochemical properties, particularly regarding absorption and emission spectra, and may thus find different applications. For our studies we have employed oxonol V (Molecular Probes, Oregon), which in our experience has the advantage of exhibiting a very stable signal with a low bleaching rate and, at the concentrations used, undetectable background signal. Another major advantage of oxonol V is that its excitation and emission wavelengths make it suitable for microscopic observation employing the rhodamine filter set. This allows the performance of double fluorescence experiments employing most common ionic probes, such as SodiumGreen (for sodium) and Fluo4 (for calcium) (Molecular Probes, Oregon, USA). Some drawbacks of oxonol V are that it is a non-ratiometric probe [31] and that calibration curves are limited to a rather narrow range of PMP values [10]. Oxonol VI has similar spectral properties to oxonol V, in addition it is ratiometric and permits to obtain reliable calibration curves [31]. This latter property may make it a convenient alternative to perform studies of the type described here.

For our experiments, oxonol V was freshly diluted in the corresponding media to a final concentration of 0.3 μM from a 0.7 mM stock solution in ethanol at 4ºC. In our experience, this stock solution remains stable for at least one year. After preloading with the oxonol solution for 30 to 60 minutes at room temperature, the coverslips bearing the BCE monolayers were mounted on a custom-made chamber (Fig. 1) loaded with the oxonol-containing solution and placed under a fluorescence microscope. In order to identify dead cells, to be discarded in the image analysis, all of the solutions incorporated into the experimental chamber contained 1 μg/ml propidium iodide (PI).

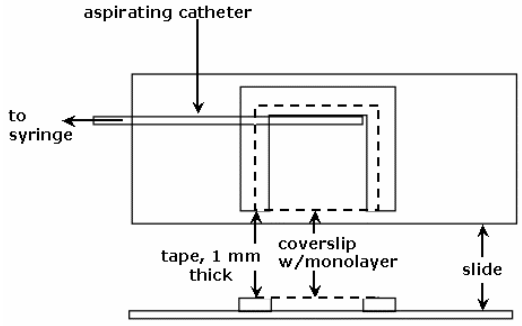

Fig. 1 Experimental chamber. Top: front view; bottom: side view. A three-sided frame made of plastic tape was stuck on a glass slide. The cells grown on a square coverslip were placed upside down on this frame. The chamber underneath the coverslip holds approximately 100 μl of medium or buffer solution. A notch on the back of the frame allows installation of a small plastic tubing. This tubing, connected to a syringe, is used to aspirate the contents of the chamber. Reproduced, with kind permission, from [25].

The fluorescent images were obtained with an epifluorescent microscope using the rhodamine filter set with a 20X or 40X planneofluor objective and photographed with a Kodak MDS120 digital camera. The camera was controlled by a computer using the MDS120 software (Kodak Digital Science) and either the Ulead Photoimpact (Ulead Systems Inc.) software or the Adobe Photoshop (Adobe Systems Inc.) software as parent application. Relative measurements of the oxonol fluorescence intensity were obtained by quantifying the average value of the red channel using the Histogram tool of the Adobe Photoshop software. The dead cells, revealed by the PI nuclear signal, were excluded from the analysis.

Empirical calibration curves for the membrane potential can be performed employing oxonol V by determining the fluorescence intensity at different external concentrations of potassium in the presence of the selective ionophore valinomycin and employing the Nernst equation [11]. In our case, the determinations of the PMP for the control conditions employing this calibration procedure yielded values in fair agreement with available experimental evidence [24].

2.3 Determination of changes in the intracellular sodium concentration

Analogously to the membrane potential, we investigated modifications in intracellular sodium concentration using the FM-IA method. For this case, we employed the fluorescent indicator sodium green tetraacetate (Sodium Green; Molecular Probes). In the corresponding experiments, the cells were incubated for 30 min at room temperature in the appropriate solution containing 5 μM Sodium Green. After washing, the coverslips were incubated in the oxonol solution containing PI and mounted in the experimental chamber (Fig. 1). The double fluorescent images obtained permitted to perform the simultaneous determination of the oxonol and Sodium Green signals. The Sodium Green fluorescent signal was analyzed employing a similar procedure to the one for the oxonol studies, but using a fluorescein filter set and selecting the green channel of the Histogram tool of the Adobe Photoshop software.

The intracellular sodium concentration $[Na^+]_i$ can be calculated from the obtained value of fluorescence intensity (F) using the following equation [32, 33]:

$$[Na^+]_i = K_d\,(F\text{-}F_{min}) \,/\, (F_{max} - F)$$

where, for room temperature, the dissociation constant (K_d) for SodiumGreen is 21 mM and F_{max} and F_{min} are the maximum and minimum fluorescence intensities, respectively. In our experiments, F_{max} was determined after incorporation of gramicidin D (1 μg/ml) to the control solutions and F_{min} was determined by replacing the total extracellular Na^+ with the non-permeant cation choline. Our studies employing this procedure yielded values in good approximation with available literature [24].

3. Results

3.1 PMP depolarization of bovine corneal endothelial cells in culture

As mentioned above, inside the cells oxonol accumulates in vesicles due to its negatively charged nature. This property determines the characteristic unevenly-distributed punctuated pattern observed in fluorescent images (Fig. 2).

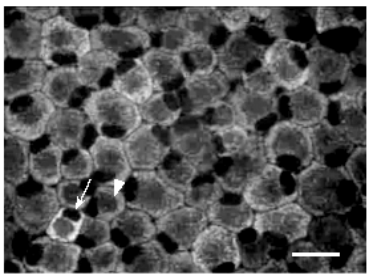

Fig. 2 Oxonol-loaded BCE cell monolayer. The arrow points to an isolated cell exhibiting a higher fluorescent signal than the rest of the cells. The arrowhead points to a juxtanuclear intracellular region with low signal intensity corresponding to areas with low vesicle densities. Note the lack of nuclear staining by PI. Bar, 30 μm. Reproduced, with kind permission, from [24].

The relative amount of oxonol in the cellular compartment varies with the PMP. An example of this property is illustrated in Figure 3, that shows the changes in the fluorescence intensity of oxonol V determined by the incorporation of gramicidin D to the bathing media of confluent corneal endothelial cells. As can be seen, gramicidin elicited a gradual increase in the oxonol fluorescence intensity that achieved its maximum at approximately 30 min. Besides this effect, shown in Fig. 3A, the image also reveals the cell remodelling characteristically produced on these cell monolayers by diverse PMP depolarizing procedures [23, 25]. Similar time courses and values of the oxonol fluorescence intensities were achieved employing both 1 and 10 μg/ml gramicidin.

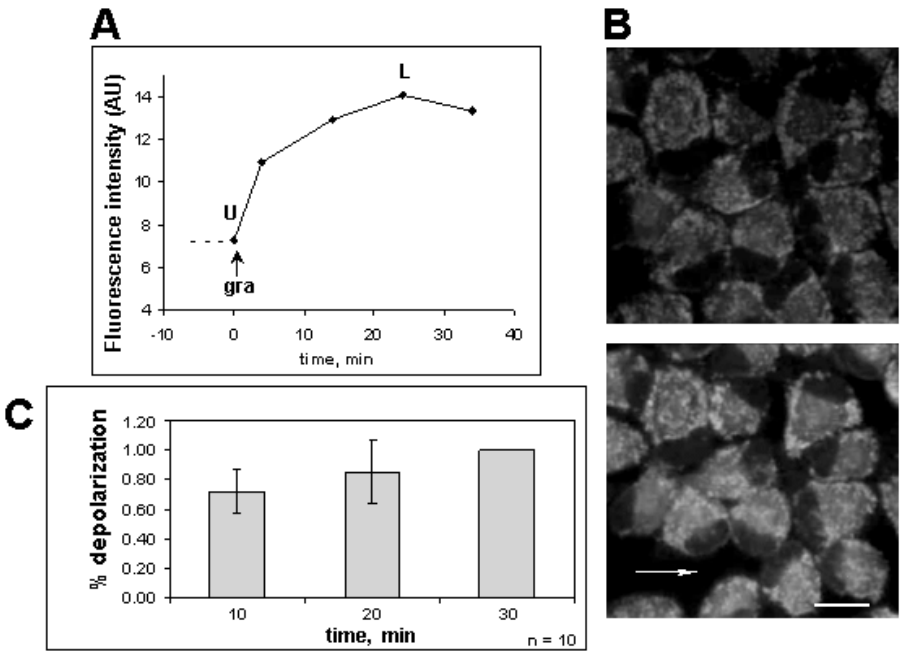

Fig. 3 Effect of gramicidin on the membrane potential of confluent corneal endothelial monolayers. (A) The plot shows the time changes in fluorescence intensity of oxonol V of a typical experiment. The cells were pre-equilibrated for 60 min in culture medium containing 0.3 μM oxonol V. Once the fluorescent signal was stable, the chamber medium was replaced by the same medium containing 10 μg/ml gramicidin D (time 0). (B) The images correspond to the same field, at time 0 (top, indicated by U on the plot) and after 25 min of incubation with gramicidin (bottom, indicated by L on the plot). The arrow shows a zone with a significant increase in intercellular space. Note the lack of nuclear staining by PI. The images shown here were obtained with longer exposure times than the ones utilized for image processing (A and C). Bar: 30 mm. (C) Relative depolarization induced by 10 μg/ml gramicidin D at different times after the incorporation of the drug. For every experiment, the depolarization produced after 30 min of treatment was taken as reference (100%). Data are means (±SD); n = 10. Reproduced, with kind permission, from [25].

Diverse other procedures determined PMP depolarization in confluent monolayers of BCE cells. Thus, the replacement of NaCl by potassium gluconate produced similar effects to those determined by gramicidin, i.e. an increase in oxonol fluorescence. Also, for cells characterized by a dominant potassium permeability and a significant chloride permeability, the replacement of extracellular chloride by a non-diffusive anion (e.g. sulfate or gluconate) should result in net KCl efflux and, consequently, in membrane depolarization. In our case, membrane depolarization was also achieved by the employment of these latter agents [25]. We could establish in this work that all of these depolarising procedures determined a characteristic reorganization of the cytoskeleton revealed, in the oxonol images, by an increase in the intracellular spaces (Fig. 3B, bottom, arrow).

3.2 PMP and intracellular sodium changes in the course of wound healing in BCE monolayers

We utilized the FM-IA method to explore whether modifications in the PMP and intracellular ionic concentrations occur during wound healing in epithelia. Our studies showed that the dramatic structural modifications undergone by the border cells in wounds produced in BCE monolayers are accompanied by changes in the PMP, as revealed by the fluorescent images of oxonol-loaded cells [24]. In this work we could establish that five minutes after injury no significant differences in oxonol fluorescence can be observed between the border cells and the cells in the rest of the monolayer, suggesting that there is no difference in the PMP between these two cell populations. Approximately 1–2 hours after wounding most of the cells at the wound border start developing an increase in oxonol fluorescence. These regions of PMP depolarization become progressively more evident and gradually acquire the shape of triangle-shaped areas with the vertices pointing towards the undamaged tissue. In later stages the increase in oxonol fluorescence extends to several rows of cells (Fig. 4, B and D).

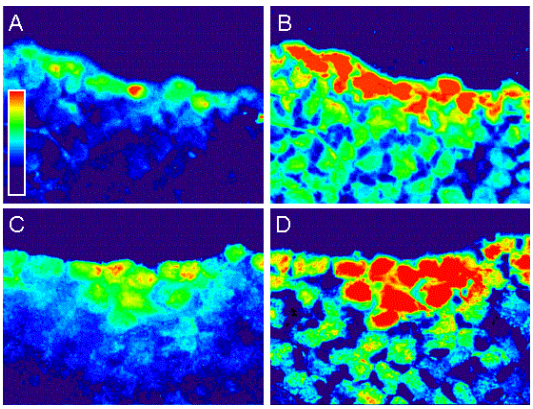

Fig. 4 Wounded monolayers were left at 37°C for the corresponding time periods; incubated in solutions containing Sodium Green tetraacetate, oxonol V, and PI; and photographed with the corresponding filters. The Sodium Green (A and C) and oxonol V (B and D) images showing the same field were processed to obtain pseudocolor images. An intensity scale is shown. Times after injury: 1 h (A and B), 2 h (C and D). Note that there is a temporospatial correlation between the depolarization area and the increase in intracellular Na^+ concentration. Reproduced, with kind permission, from [24].

To assess whether the PMP depolarization observed at the border cells is a consequence of an increase in sodium permeability, we performed double-staining experiments to simultaneously study the time course of the oxonol and sodium signals during the healing process. The images shown in Fig. 4 indeed reveal that, concomitantly to the plasma membrane depolarization, there is an increase in intracellular sodium in the cells at the wound borders. This increased signal of the sodium concentration propagates towards the rest of the monolayer following the same pattern observed for PMP depolarization.

4. Final remarks

In this chapter we have made a short revision of the use of fluorescent probes in the determination of changes in the plasma membrane potential, have briefly described the method of study of these changes employing standard fluorescent microscopy and image analysis, and have illustrated this method with examples from work performed by us on corneal endothelial cells in culture. We have particularly focused on the employment of some members of the oxonol family as potentiometric probes. Some major advantages of oxonols are that, due to their anionic nature, they permit to discriminate the PMP signal from other possible sources, such as mitochondria, and that some of them yield reliable calibration curves. Due to their characteristic absorption and emission wavelengths, oxonol V and VI are suitable for the performance of double fluorescence studies in simultaneous combination with fluorescent probes with different spectral properties, such as those commonly utilized to asses the intracellular concentrations of sodium or calcium. In particular, oxonol V displays a remarkably stable fluorescent signal with a very low bleaching rate. Although non-ratiometric and not easy to calibrate, in our experience it has resulted a most valuable tool for the studying of relative modifications in the PMP.

Acknowledgements The supports by CSIC and PEDECIBA (Universidad de la Republica, Uruguay) and by DYNACIT (PDT 54/016), Ministerio de Educación y Cultura, Uruguay) are gratefully acknowledged.

References

[1] S.G. Schultz, Am J Physiol **241,** F579 (1981)
[2] A.M. Weinstein, Bull Math Biol **59,** 451 (1997)
[3] J.A. Hernandez and E. Cristina, Am J Physiol **275,** C1067 (1998)
[4] W.D. Stein, Int Rev Cytol **215,** 231 (2002)
[5] M. Olivotto, A. Arcangeli, M. Carla, and E. Wanke, Bioessays **18,** 495 (1996)
[6] S.N. Orlov and P. Hamet, J Membr Biol **210,** 161 (2006)
[7] E. Carafoli, Febs J **272,** 1073 (2005)
[8] J. Plasek and K. Sigler, J Photochem Photobiol B **33,** 101 (1996)
[9] M. Zochowski, M. Wachowiak, C.X. Falk, L.B. Cohen, Y.W. Lam, S. Antic, and D. Zecevic, Biol Bull **198,** 1 (2000)
[10] J.P. Kukkonen, R. Hautala, and K.E. Akerman, Neurosci Lett **212,** 57 (1996)
[11] A.S. Waggoner, Annu Rev Biophys Bioeng **8,** 47 (1979)
[12] C.L. Bashford, Biosci Rep **1,** 183 (1981)
[13] H.A. Wilson, B.E. Seligmann, and T.M. Chused, J Cell Physiol **125,** 61 (1985)
[14] C.L. Bashford and C.A. Pasternak, Biochim Biophys Acta **817,** 174 (1985)
[15] F. Di Virgilio, P.D. Lew, T. Andersson, and T. Pozzan, J Biol Chem **262,** 4574 (1987)
[16] B. Ehrenberg, V. Montana, M.D. Wei, J.P. Wuskell, and L.M. Loew, Biophys J **53,** 785 (1988)
[17] T.R. Cheek, A. Morgan, A.J. O'Sullivan, R.B. Moreton, M.J. Berridge, and R.D. Burgoyne, J Cell Sci **105 (Pt 4),** 913 (1993)
[18] K. Shin, V.C. Fogg, and B. Margolis, Annu Rev Cell Dev Biol **22,** 207 (2006)
[19] M. Cereijido, R.G. Contreras, and L. Shoshani, Physiol Rev **84,** 1229 (2004)
[20] V. Montana, D.L. Farkas, and L.M. Loew, Biochemistry **28,** 4536 (1989)
[21] V. Dall'Asta, R. Gatti, G. Orlandini, P.A. Rossi, B.M. Rotoli, R. Sala, O. Bussolati, and G.C. Gazzola, Exp Cell Res **231,** 260 (1997)
[22] T.J. Rink, C. Montecucco, T.R. Hesketh, and R.Y. Tsien, Biochim Biophys Acta **595,** 15 (1980)

[23] S. Chifflet, V. Correa, V. Nin, C. Justet, and J.A. Hernandez, Exp Eye Res **79,** 769 (2004)
[24] S. Chifflet, J.A. Hernandez, and S. Grasso, Am J Physiol Cell Physiol **288,** C1420 (2005)
[25] S. Chifflet, J.A. Hernandez, S. Grasso, and A. Cirillo, Exp Cell Res **282,** 1 (2003)
[26] T.F. Weiss, *Cellular biophysics*. Vol. 1: Transport, 1996, Cambridge, Mass.: MIT Press, pp. 532-533.
[27] D.J. Aidley and P.R. Stanfield, *Ion channels: molecules in action*. 1996, Cambridge; New York: Cambridge University Press, pp. 115–116.
[28] I. Johnson, Histochem J **30,** 123 (1998)
[29] C.L. Bashford and J.C. Smith, Methods Enzymol **55,** 569 (1979)
[30] H.J. Apell and B. Bersch, Biochim Biophys Acta **903,** 480 (1987)
[31] A. Holoubek, J. Vecer, M. Opekarova, and K. Sigler, Biochim Biophys Acta **1609,** 71 (2003)
[32] J. Li, J. Eygensteyn, R. Lock, S. Bonga, and G. Flik, J Exp Biol **200,** 1499 (1997)
[33] J.L. Winslow, R.L. Cooper, and H.L. Atwood, J Neurosci Methods **118,** 163 (2002)